Engineering Structures 338 (2025) 120607

Contents lists available at ScienceDirect

Engineering Structures

journal homepage: www.elsevier.com/locate/engstruct

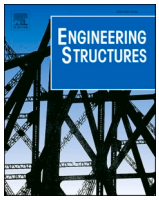

A generalised framework for designing topological interlocking structures from monomorphic elements

Siya Wang [a], Xiaoshan Lin [a,*], Y.X. Zhang [b], Yi Min Xie [a,c]

[a] Centre for Innovative Structures and Materials, School of Engineering, RMIT University, Melbourne, VIC 3000, Australia
[b] School of Mechanical and Mechatronic Engineering, University of Technology Sydney, NSW 2007, Australia
[c] College of Future Technologies, Hohai University, Changzhou, Jiangsu 213200, China

ARTICLE INFO

Keywords:
Topological interlocking
Parametric design
Monomorphic element
Curved contact surface
Interlocking mechanism

ABSTRACT

Topological interlocking (TI) structures, known for their superior energy dissipation, damage tolerance, and adaptability, are gaining increasing attention as innovative solutions to advanced structural designs. In this study, a general framework is developed for designing TI elements with curved contact surfaces, enabling the creation of monomorphic elements through a matched concavo-convex interface. The element shapes are controlled by parameters such as polygon type, polygon length, curve function, and element thickness. This approach can be applied to designing TI elements for both planar and non-planar structures. Validation is achieved through the design of 24 planar and 12 non-planar TI elements, along with two 3D-printed prototypes. Furthermore, the impact performance of typical TI plates is compared to that of a monolithic structure to demonstrate the effectiveness of the generalised interlocking mechanism.

1. Introduction

Topological interlocking (TI) structures consist of elements that interlock through kinematic constraints arising from their geometric design and mutual arrangement. This design principle eliminates the need for external connectors or binders, as each element is held in place by constraints from neighbouring elements. When the assembly is constrained at the periphery, each element becomes securely locked in place, with geometry and interfacial contact ensuring structural integrity. This interlocking mechanism enhances structural robustness [1], localises failure [2], and enables element replacement, making TI structures highly sustainable and resilient [3]. Additionally, their segmented nature allows for superior energy absorption [4,5] and vibration attenuation under dynamic loads [6]. TI structures also exhibit strong tolerance to missing elements, maintaining structural functionality even when certain elements are removed [7]. These advantages make TI structures promising for civil engineering applications, such as retaining walls [8], pavement blocks [9], seismic-resistant members [10], and tunnel shielding [11].

Classical TI elements can be categorised into two main families. The first consists of polyhedra derived from convex polygons, while the other features curved contact surfaces, such as osteomorphic elements [12]. The two types of TI elements employ distinct methods to control their morphology and achieve the interlocking effect. Polyhedral TI elements are shaped by geometric principles. The movement of the central element is constrained by neighbouring elements due to the reciprocal movement tendencies of their lopsided planes. These elements can be arranged in a checkerboard pattern to form a planar structure, with adjacent elements featuring mutually perpendicular frictional contact planes [13]. The example of a tetrahedral TI structure is illustrated in Fig. 1(a). The middle sectional plane displays a regular tiling with reciprocal inclined plane directions in the contact area, which makes the centre element interlocked by its neighbouring elements. Dyskin et al. [14] discovered that identical elements in the shape of five platonic bodies (tetrahedron, cube, octahedron, dodecahedron, and icosahedron) can be assembled into planar structures with topological interlocking features. Later, a series of indentation tests were carried out by Dyskin et al. [14] to study the mechanical behaviour of polyhedral TI structures assembled from the tetrahedral and cubic elements. The results indicated that these structures were highly flexible and exhibited a strong tolerance for missing elements. Weizman et al. [15] developed polyhedral TI plates using semi-regular and non-regular tiling, which involve combinations of two or more regular polygons and identical irregular polygons respectively, to explore their potential applications in

* Corresponding author.
E-mail address: susanna.lin@rmit.edu.au (X. Lin).

https://doi.org/10.1016/j.engstruct.2025.120607
Received 4 February 2025; Received in revised form 12 April 2025; Accepted 16 May 2025
Available online 24 May 2025

architectural design, emphasising their advantages in reusability and damage tolerance. Additionally, Bejarano and Hoffman [16] proposed an algorithm to automatically generate TI structures with tetrahedral configurations using square tiling. The geometry of the element was controlled by its height and centre point. The tetrahedral TI element was applied to non-planar surfaces, such as cylindrical, spherical, and torus surfaces, using shape generation with a square mesh. However, the design options were limited due to the difficulty in calculating the effective interlocking inclination angle [16].

Dyskin et al. [2] proposed the first TI element with curved interfaces, an osteomorphic element featuring two-sided curved surfaces with a concavo-convex morphology. By aligning the protrusions and recesses of osteomorphic elements, they could be assembled into a structural unit, as depicted in Fig. 1(b). The morphology of osteomorphic elements was defined using mathematical functions that meet symmetry, periodicity, and surface contact conditions [2]. The interlocking mechanism of osteomorphic elements resulted from the mutual jamming of protrusions and recesses on their contact surfaces under a confining load. Experimental tests and numerical simulations reported by Dyskin et al. [17] demonstrated that TI structures with curved interfaces created flexible, failure-tolerant structures capable of creating multi-layer configurations. Inspired by the work of Dyskin et al. [2], Rezaee Javan et al. [18] proposed a TI element with a four-sided curved interface, exhibiting enhanced impact energy absorption capacity compared to osteomorphic elements. Their experimental results demonstrated that the interlocking assembly plates exhibited significantly enhanced flexural performance and a localised failure mode, in contrast to the brittle-dominated behaviour observed in monolithic plates [18]. Additionally, Akleman et al. [19] developed a method to generate TI elements with larger curved contact areas using wallpaper patterns and fabric textures. TI elements with curved contact surfaces reduce the reliance on frictional contributions compared to polyhedral TI structures, thereby broadening the scope of applications for TI structures [20]. Recently, more alternative TI element designs have been proposed. For example, Koureas et al. [21] investigated the effect of hierarchical interlocking on beam-like topologically interlocked structures. Their research showed that introducing sinusoidal surface alterations to planar-faced blocks could significantly enhance the interlocking performance. Dalaq and Barthelat [22] studied the structural behaviour of segmented beams composed of rigid elements under transverse forces, starting with simple cube geometries and subsequently enhancing the interfaces using two-dimensional polynomial functions. Test results for the ceramic glass segmented beams revealed that the enhanced blocks transformed brittle failure into graceful progressive deformation, achieving toughness 370 times greater than that of monolithic structure while retaining 40 % of its strength. However, previous TI elements were primarily derived based on square tiling and applied to planar structures. Xu et al. [23] proposed a non-planar TI element with curved contact surfaces, based on hexagonal tiling, for tubular structures by morphing a planar structure into a cylindrical surface, representing one of the few studies on non-planar TI elements. The tubular structure assembled with these TI elements demonstrated greater energy absorption capacity and a more localised failure pattern compared to both monolithic structure and the structure assembled with traditional elements. This configuration shows potential for use in tunnel segments, where the surrounding soil pressure can effectively provide the necessary confining load. Currently, the design alternatives for elements with curved contact surfaces are limited, and it is difficult to link shape morphology with design parameters using the methods in existing studies.

Although previous studies have made progress in the development of TI structures and concluded that polygon tiling provides the geometric foundation [26,27], they primarily focused on regular or semi-regular tilings, leaving many other tiling options unexplored. Moreover, the existing designs for TI elements are limited, with the majority focusing on polyhedral planar structures that heavily rely on material friction, hindering the broader application of TI structures. Besides, the relationship between the interlocking effect and surface morphology remains unclear for elements with curved interfaces generated using existing methods in the literature. At present, there is a lack of a general method for generating TI elements with various designs that can meet diverse performance demands.

In this study, a generalised approach is developed for designing TI elements with curved contact surfaces, applicable to both planar and cylindrical structures. By employing appropriate curve functions, such as sinusoidal functions, the framework generates precisely matched concavo-convex interfaces to achieve interlocking. The parametric design enables control over shape morphology using polygonal prototiles, curve functions, and element dimensions. Unlike previous approaches that produce isolated TI cases, this method systematically generates an entire family of TI elements. These elements feature monomorphic prototile characteristics, which enhance manufacturability, construction efficiency, and recyclability. The effectiveness of the proposed framework is demonstrated by examples of TI elements created based on different plane tilings. Finally, the impact performance of typical planar TI structures is compared to that of a monolithic plate to highlight the benefit of the interlocking mechanism.

2. General framework for creating TI structures

In this section, a systematic approach is developed for creating TI elements characterised by curved interfaces. The generated elements can be assembled into planar structures and have the potential to extend

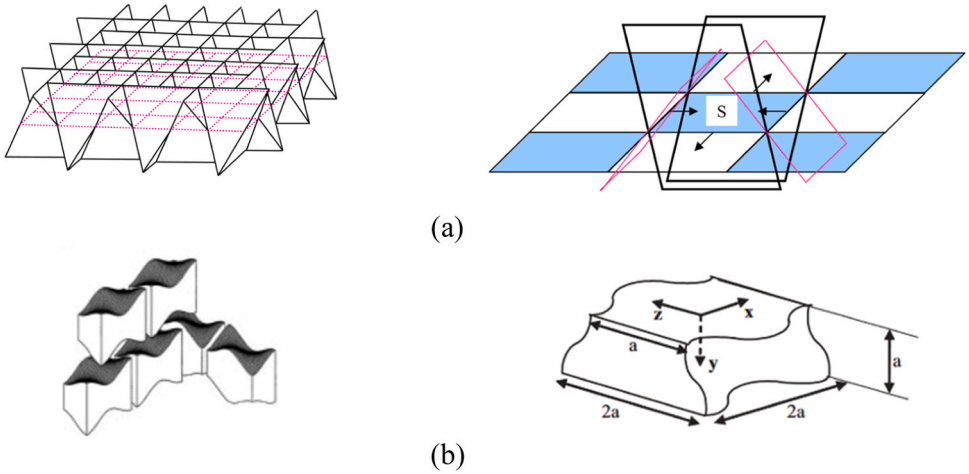

Fig. 1. Examples of two typical TI element families: (a) tetrahedral TI elements [24], and (b) osteomorphic TI elements [2,25].

into non-planar forms, such as tubular structures, while preserving their monomorphic feature. The developed framework can be implemented using the 3D geometric modelling software Rhino to create TI elements.

2.1. Selection of polygon tiling

In the past, a variety of TI elements have been introduced in the literature [2,14,18,23,27–30], all sharing the ability to completely cover a flat surface with non-overlapping figures. This study expands the design options for TI elements by using tilings that have not been explored in previous research. In the classical book by Grunbaum and Shephard [31], a wide range of plane tilings has been discussed. In this study, four representative types of polygon tilings from their work are selected as the basis for generating TI elements, considering design and construction simplicity: regular tiling, parallelogram tiling, Laves tiling, and brick wall tiling, as shown in Fig. 2. The selected tilings consist of tiles that are identical in size and shape, resulting in a monomorphic prototile. This simplifies manufacturing and construction by enabling single moulding and straightforward assembly.

As shown in Fig. 2(a), regular tiling consists of identical regular polygons, such as equilateral triangles, squares, and hexagons. Parallelogram tiling, depicted in Fig. 2(b), is created using irregular four-sided polygons. Brick wall tiling reported in [32] provides another monomorphic design option, allowing the prototile to cover a plane using various laying arrangements, as shown in Fig. 2(c). Brick wall tiling is not edge-to-edge, as the long side of a rectangle tile is shared by two adjacent tiles. Therefore, the curve function for brick wall tiling requires special attention. The ratio of the shorter side to the longer side should align with the ratio of protrusions and recesses to ensure a snug fit in the plane tiling. Fig. 2(d) shows eight Laves tilings selected for their monomorphic prototile and edge-to-edge characteristics. Regular tiling, parallelogram tiling, and Laves tiling are edge-to-edge, i.e. adjacent tiles share a complete side, which ensures a compatible concavo-convex relationship between the edges of the tiles.

2.2. Creating interlocking effect for polygonal prototile

In this study, curvature is introduced to the prototile edges to create an in-plane interlocking effect. The reciprocal local curvature of the matched edges prevents the in-plane movement of the elements. The curved edges also form the basis for creating a concavo-convex contact surface between elements, which is crucial for resisting out-of-plane movement. A sinusoidal function, as given in Eq. (1), is used to generate curvature for prototile edges (Fig. 3).

$$f(x) = \mathrm{Asin}(k\frac{\pi x}{a}), k\epsilon Z \tag{1}$$

where x is the position along the edge; A is the amplitude, representing the peak deviation of the curve from the edge; k is the wave number, which controls the number of protrusions and recesses, and k must be an integer; a refers to the edge length.

The curvature direction and shape, controlled by the amplitude and wave number, are critical for achieving non-overlapping plane tiling. Depending on the period of the sinusoidal function, the edge shape can be classified as half-wave shape and full-wave shape, as shown in Fig. 4 (a). The half-wave shape exhibits reflective symmetry about the perpendicular bisectors, while the full-wave shape has 180-degree rotational symmetry about its midpoint. Since the resulting prototile, with edges featuring protrusions and recesses, can only cover the plane when the number of protrusions is equal to that of recesses, half-wave shapes must be excluded for prototiles with an odd edge number [33]. This is because their edges would inevitably have mismatched protrusions and recesses. For prototiles with an even edge number, employing a half-wave shape requires dividing the edges into two

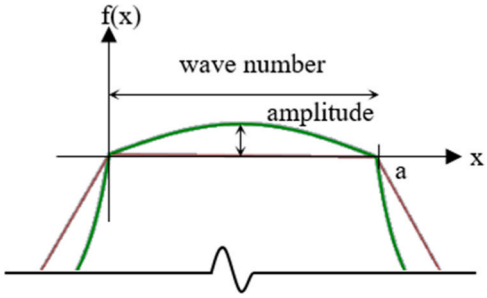

Fig. 3. Introduction of curvature to prototile edges.

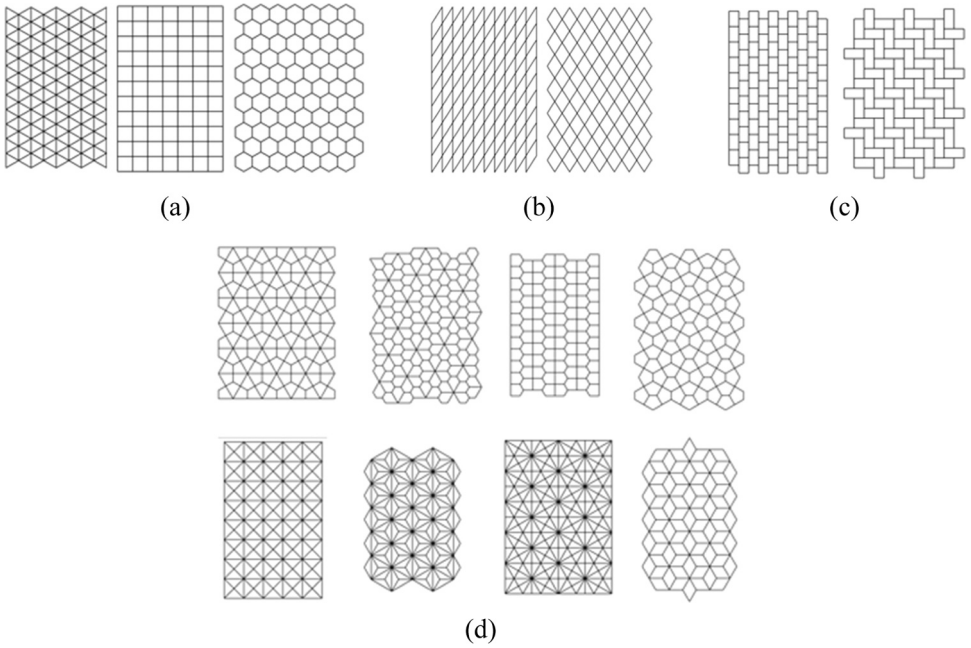

Fig. 2. Four plane tiling types as foundations for TI elements: (a) regular tiling [31], (b) parallelogram tiling [31], (c) brick wall tiling [32], and (d) irregular Laves tiling [31].

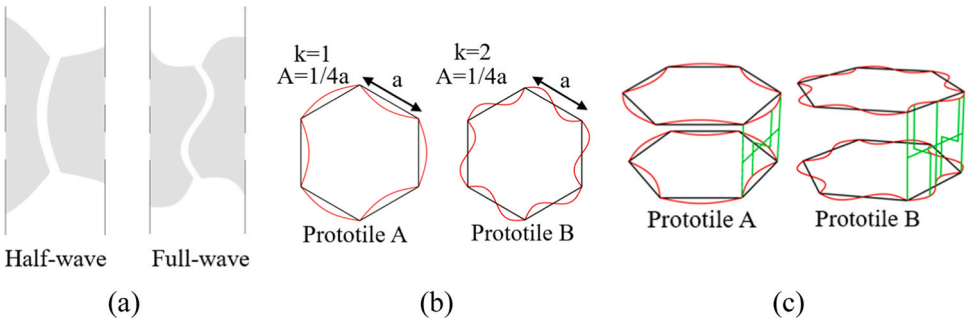

Fig. 4. Process of generating curvature for prototile edges: (a) edge matching rules, (b) prototiles with edges modified using sinusoidal function, where a refers to polygon length and k refers to the wave number (Prototile A: $A = 1/4a, k = 1$, half-wave; Prototile B: $A = 1/4a, k = 2$, full-wave), and (c) curved edges for the top and bottom surfaces of TI elements.

groups. These groups must have opposite convexities, determined by the positive or negative amplitude value, to ensure a balance in the number of protrusions and recesses. For the full-wave shape, the edge-matching rule is naturally satisfied without the need to adjust the amplitude. Fig. 4 (b) shows examples of transforming a regular hexagonal prototile into ones with curved edges, featuring half-wave shape (Prototile A) and full-wave shape (Prototile B).

The out-of-plane interlocking of the TI structure is attained through matched concavo-convex surface morphology between neighbouring elements. This surface morphology is achieved by ensuring that the curved edges on the top and bottom surfaces of the element have reflective convexity, as shown in Fig. 4(c). The green lines serve as auxiliary lines, indicating the reflective relationship between the curved edges on the top and bottom surfaces. The creation of interlocking interface for TI elements will be discussed in detail in Section 2.3.

The function used to generate curved edges could be any function that produces the concavo-convex property, such as the circular curve employed by Yong [6] to create osteomorphic elements. The selection of the sinusoidal function in this study is motivated by three key factors. Firstly, the shape generated by this function perfectly aligns with the concavo-convex profile required for TI elements. Secondly, in previous studies, such as the one reported by Weizmann et al. [27], polylines arranged in a zig-zag pattern were used, forming triangular or rectangular interfaces. However, the sinusoidal function offers a smoother profile, which reduces stress concentration at the contact areas between elements, as shown in Fig. 5. Additionally, the sinusoidal function is one of the simplest periodic curve functions, providing a straightforward relationship between the curve's shape and its parameters.

2.3. Creating interlocking interface for TI elements

In this study, the contact surfaces of the TI elements are generated and controlled using the curved prototile edges on the top and bottom surfaces, by employing the "loft" function in Rhino. The generated interfaces are ruled surfaces, formed by a continuous series of straight-line segments connecting the curved prototile edges, as illustrated by the yellow isocurves in Fig. 6(a). By applying the loft function to each pair of top and bottom curved prototile edges, interlocking interfaces are

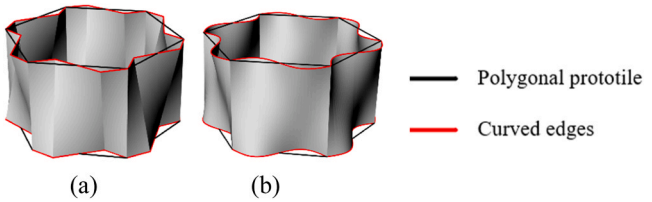

Fig. 5. Interfaces with different curve functions: (a) polylines and (b) sinusoidal function.

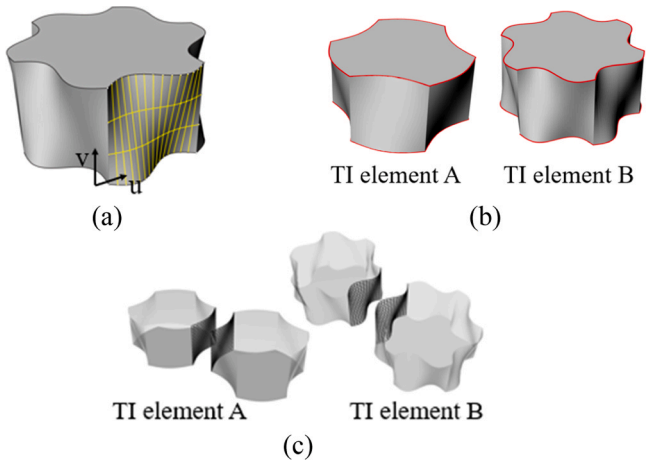

Fig. 6. Generating TI elements: (a) formation of interfaces in TI elements, (b) TI element A and TI element B, and (c) paired elements with matched concavo-convex interfaces.

created. Fig. 6(b) shows the examples of TI elements (TI element A and TI element B) generated from Prototile A and Prototile B.

Fig. 6(c) illustrates the matched concavo-convex contact surfaces of pairs of elements, where the protrusions of one element fit into the recesses of the other, and vice versa. When a confining boundary is applied to compress the assembly, these complementary surfaces effectively restrict out-of-plane movement. The interlocking effect is achieved through both the material jamming between protrusions and recesses as well as the frictional resistance at the interfaces. In contrast to polyhedral TI elements, friction plays a secondary role compared to geometric constraints.

2.4. Non-planar TI elements

The planar TI elements generated by the proposed method can be adapted to create non-planar elements for shell structures using the "FlowAlongSrf" function in Rhino. This function transforms an object from a source plane to a target surface, as demonstrated by Xu et al. [23]. The effectiveness of this method lies in the resulting non-planar TI elements, which retain their monomorphic characteristics and interlocking effect. However, not all TI elements are compatible with this method. To ensure interlocking and monomorphic features in the resulting non-planar TI elements, two criteria must be met: 1) the target surface must be developable and with uniform curvature, and 2) the prototiles are isotropic in the uv plane directions, i.e., the prototiles are arranged translationally along the u and v directions, ensuring that the size of each element remains consistent in these directions, as illustrated in Fig. 7.

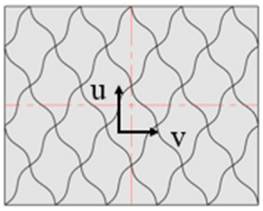

Fig. 7. Example of TI assembly with isometric prototiles in the *uv* plane directions.

2.4.1. Cylindrical target surface

To transform planar geometry onto cylindrical surfaces, the "FlowAlongSrf" in Rhino is employed. This tool constructs a precise map f between the plane and the target surface, as demonstrated in Fig. 8, ensuring that the intrinsic properties of the geometry, such as distances and angles, are preserved. When used with cylindrical surfaces, which are developable surfaces with uniform curvature, the function guarantees that the transformed TI elements retain their monomorphic features, making it ideal for creating tubular or arch designs. This capability enables the accurate and efficient morphing of planar TI elements onto cylindrical surfaces, preserving both their interlocking interfaces and monomorphic characteristics.

2.4.2. Isometry of prototile arrangement

Fig. 9(a) shows two tubular assemblies transformed from planar TI structures through morphing. TI element A originates from hexagon tiling, while TI element C is derived from square tiling. Both element types feature half-wave curved edges. Fig. 9(b) compares the dimension and curvature of the non-planar TI elements with their planar prototypes before transformation. It can be observed that the non-planar element derived from the TI element A retains the monomorphic feature, while the one from the TI element C does not. Before transformation, both TI elements A and C exhibit monomorphic features. In both types, the adjacent elements have identical dimensions of 3.6 mm and zero curvature. After transformation, the curves in adjacent TI element A experience a uniform stretch to 3.9 mm and gain a consistent curvature of $1/r$ (where r is the radius of the cylinder), thus preserving the monomorphic feature. Conversely, for TI element C, the adjacent elements are not isometric in the v direction due to a 90° rotation of the right element relative to the left. After morphing, the different deformation scales in the u and v directions result in variations in dimension and curvature. Specifically, the curve of the right element retains its original dimension of 3.6 mm and zero curvature in the v direction, while the left element's curve stretches to 4.7 mm and acquires the curvature of the cylindrical surface as $1/r$ in the u direction. Unlike the assembly formed by TI element A, the arrangement of TI element C does not satisfy the isometry requirement. Consequently, differences in dimensions and curvature after the mapping prevent it from preserving the monomorphic characteristic. Therefore, to achieve non-planar TI structures, planar TI elements must fulfil the isometry requirement in both directions.

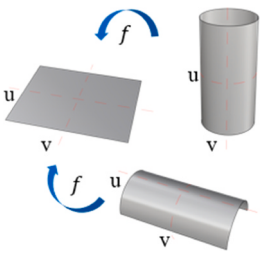

Fig. 8. Mapping planar geometry onto cylindrical surfaces.

2.5. Summary of design framework

The framework developed in this study for designing TI structures with monomorphic prototiles featuring curved interfaces involves three main steps: 1) selecting a 2D polygonal tiling that inherently possesses monomorphic characteristics, 2) shaping the contact edges to create concavo-convex features with an equal number of protrusions and recesses, and 3) constructing interlocking interfaces based on curved edges. To create cylindrical structures, the configuration of planar TI elements must satisfy the isometry requirement in the *uv* directions. The morphology of TI elements is governed by four design parameters, including polygonal prototile, polygon length, curve function, and element thickness, as demonstrated in Fig. 10. The design workflow is outlined in Fig. 11.

3. Validation of the proposed framework

3.1. New TI elements developed using the proposed framework

In this study, the four typical polygon tilings introduced in Section 2.1 are employed to generate new TI elements. In these examples, the curve function has a consistent amplitude set to a quarter of the square length a, as shown in Fig. 12. By implementing the proposed methodology to the four types of plane tilings, 24 planar TI elements are generated, as depicted in Fig. 12, along with their corresponding polygonal prototiles and curve functions. The assembled planar structures consist of both complete and truncated elements: the elements at the plate boundary have to be cut to conform to the straight edges. The primary distinctions among these TI elements lie in the polygonal prototiles and the curve functions used to generate various element geometries and interface morphologies. Notably, in the case of the triangular prototile, the half-wave function is excluded due to its tendency to create an imbalance between the number of protrusions and recesses. When the half-wave function is employed in the elements with even edges, the polygon edges are designed to have different convexity to ensure an equal number of protrusions and recesses in the plane. The concavo-convex interface morphology, as shown in the paired TI elements in Fig. 12, is formed by lofting the matched top and bottom edges with opposing convexities. The TI structures are then created by assembling the TI elements according to their matching shapes.

Among the 24 planar TI assemblies, half exhibit isometry in the *uv* directions, as indicated by the red dash lines in Fig. 13(a). Along these lines, the neighbouring elements are arranged isometrically, either translationally or reflectively, ensuring that each element experiences consistent deformation along these directions during morphing. These assemblies can be transformed into non-planar structures based on a cylindrical surface. Fig. 13(b) illustrates two examples of transformed structures and their non-planar prototiles TI element D and TI element E, representing arch and tubular structures. As can be seen, the two non-planar TI structures exhibit matched curved interfaces and isometry arrangement in the *uv* directions after transformation. The two structures maintain both the interlocking effect and monomorphic properties.

3.2. 3D printed prototypes

To further demonstrate the effectiveness of the proposed framework in generating TI elements, two prototypes are fabricated using 3D printing technology. The planar structure is designed based on regular square tiling, while the tubular structure is derived from rectangular parallelogram tiling. The TI elements are produced using a liquid-crystal display (LCD) resin printer and then assembled into a planar structure measuring 50 × 50 × 25 mm and a non-planar structure measuring D50 × L50 × T25 mm.

LCD 3D printing technology is an advanced resin-based 3D printing method that uses a digital screen to control UV light exposure on a photopolymer resin, enabling highly detailed and precise 3D prints.

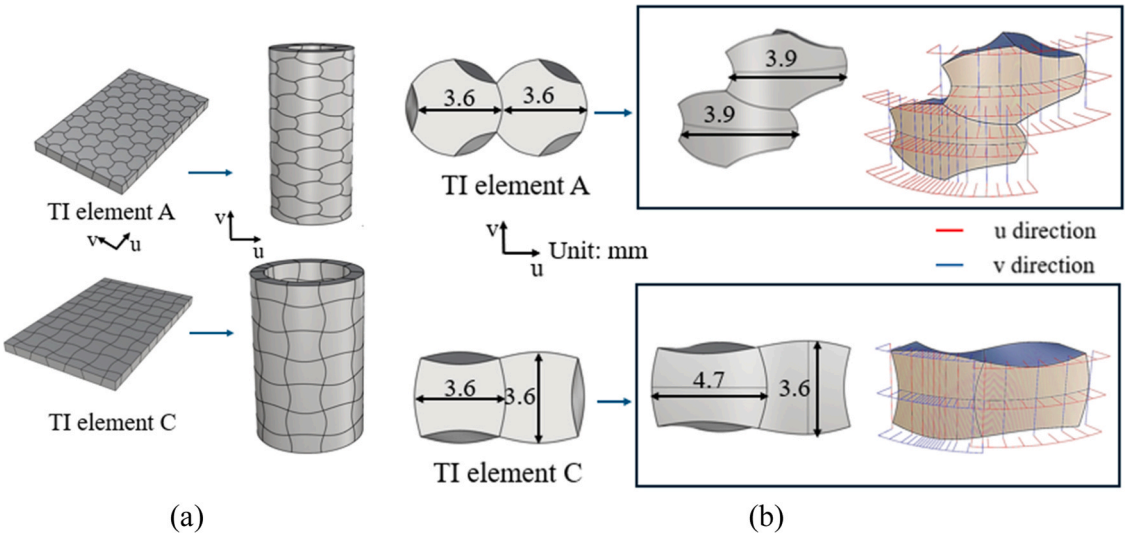

Fig. 9. Morphing process: (a) converting planar TI structures to tubular structures, and (b) comparison of dimension and curvature in *uv* directions.

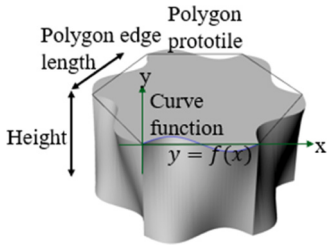

Fig. 10. Design parameters.

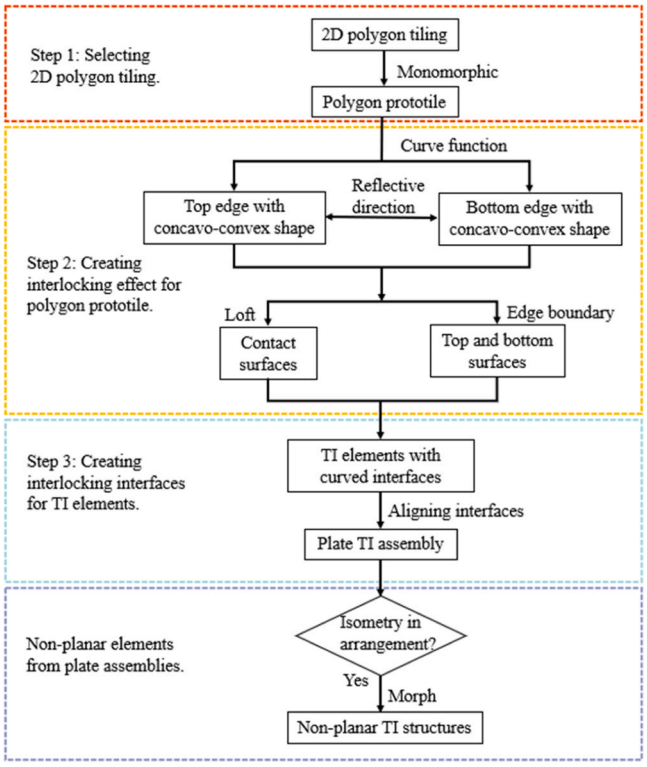

Fig. 11. Design framework for TI structures.

Similar to SLA (Stereolithography) and DLP (Digital Light Processing) technologies, it utilises a liquid crystal display to mask and project the image of the model layer by layer. In this study, the Anycubic Photon M3 Max 3D printer is employed for its high precision and large build volume, making it ideal for fabricating detailed components. The printer is equipped with a high-resolution monochrome exposure screen and a parallel matrix light source, ensuring uniform exposure and accurate printing [34]. For materials, UV resin is selected for its compatibility with the printer's 365–410 nm UV wavelength range. Critical printing parameters are carefully controlled to achieve optimal results. The printing speed is maintained below 6 cm/hr to ensure high precision, with the bottom exposure time set to 30 seconds and regular exposure time to 3 seconds. The layer thickness is set at 0.05 mm.

Figs. 14(a) to 14(c) show the printed planar elements and their assembly. During the assembly of the planar TI structure, all elements are arranged on a working plane based on the protrusions and recesses of the elements. By applying a frame as the boundary, the TI elements match seamlessly, resulting in a tightly compacted planar structure. The movement of each element is restrained by the geometrical constraint imposed by the neighbouring elements, creating an interlocking effect.

Figs. 14(d) to 14(f) show the printed non-planar TI elements and the assembled tubular TI structure. During the assembly of the non-planar TI structure, a PVC tube support is used to provide a cylindrical base surface for positioning the non-planar elements. The boundary of the non-planar TI structure is then secured with a rubber band, as shown in the figure. Once the boundary confinement is applied, the PVC tube is removed, and the assembly remains stable, demonstrating the efficacy of the interlocking effect.

It can be seen that the interlocking mechanism is effective in both planar and non-planar TI structures, where the curved contact surfaces and the unique geometry of the elements ensure structural integrity. In assemblies constrained at the periphery, each element is locked in place, enabling the structure to resist gravity and multi-directional motions. This stability, even under tilting or external motion, is attributed to the geometric constraints imposed by neighbouring elements. The authors' previous experimental studies [18,23] on the impact performance of planar and tubular TI structures with curved interfaces further support these findings, demonstrating that structural stability remains unaffected by the movement of testing specimens, as each element remained securely interlocked within the assembly [23,28]. While confinement is critical for activating and maintaining the interlocking mechanism, it does not necessarily require fixed external devices. In practice, sufficient confinement can be achieved through passive means inherent in existing loading scenarios, such as the self-weight or external pressures. As

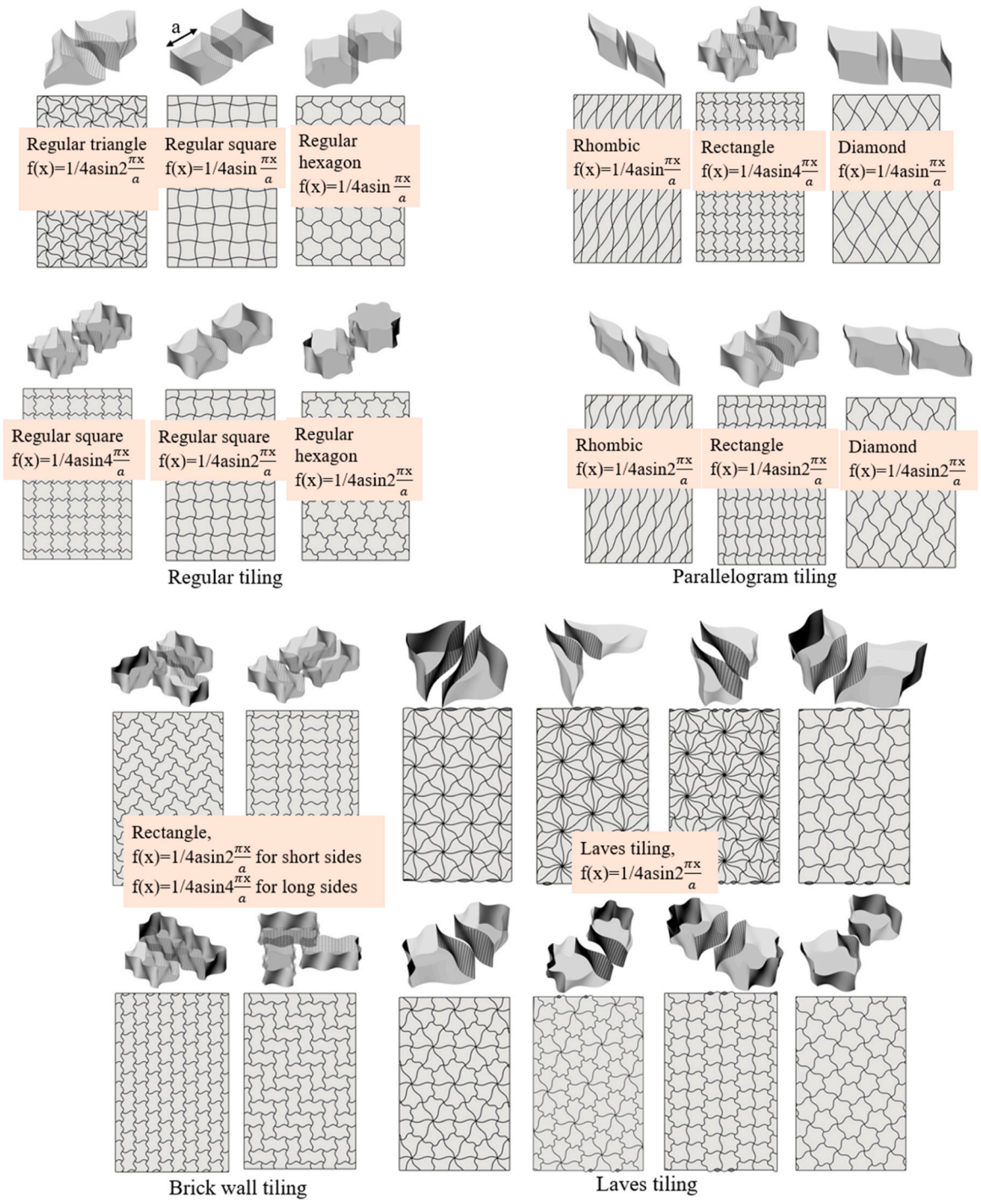

Fig. 12. Twenty-four planar TI structures and their paired prototiles (*a*: the length of square prototiles).

demonstrated in [23,28], such passive loading conditions are adequate to sustain the mechanical engagement of TI structures, enabling practical applications without the need for continuous external restraint.

In this study, the prototypes have been produced on a small scale. Although the physical models primarily demonstrate shape morphology and do not undergo structural performance testing, the manufacturing and assembly methods described provide valuable guidance for producing and constructing TI structures. Manufacturing tolerances, which can influence assembly fit and mechanical performance, are excluded from the current scope to maintain clarity in the development of the design methodology and to avoid confounding factors in the interpretation of interlocking effects. Future work may consider tolerance-informed design, incorporating probabilistic modelling or experimental validation to assess the robustness of TI structures under real-world fabrication constraints.

3.3. Impact performance and interlocking mechanism

This section examines the impact performance of TI plates, highlighting the interlocking mechanism through a comparison with conventional monolithic design. Three typical planar TI elements, derived from regular triangle, square, and hexagon, are selected for the analysis. All elements are made of concrete. The TI element created based on square tiling serves as the reference, characterised by an edge length of

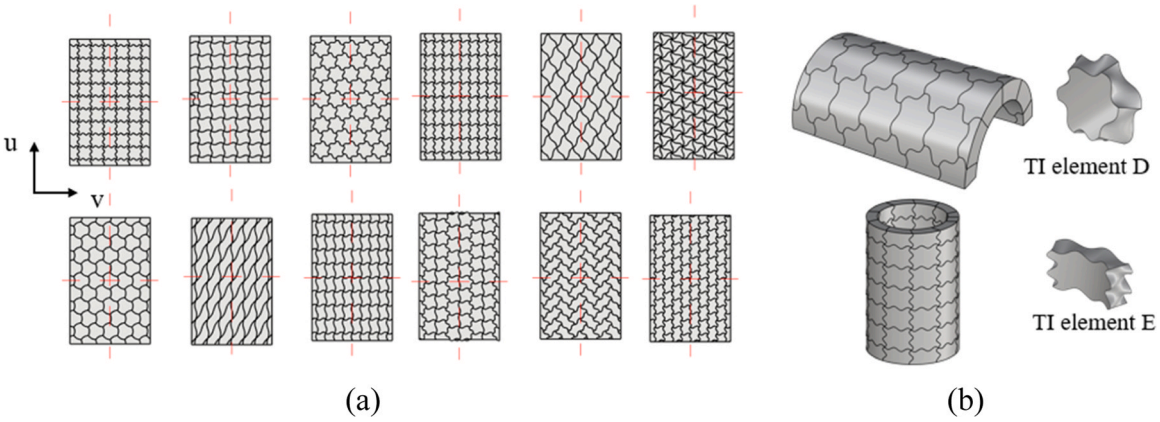

Fig. 13. Twelve transformable planar assemblies and post-transformed examples (a) planar structures that meet the isometry requirement, and (b) two examples of non-planar TI structures.

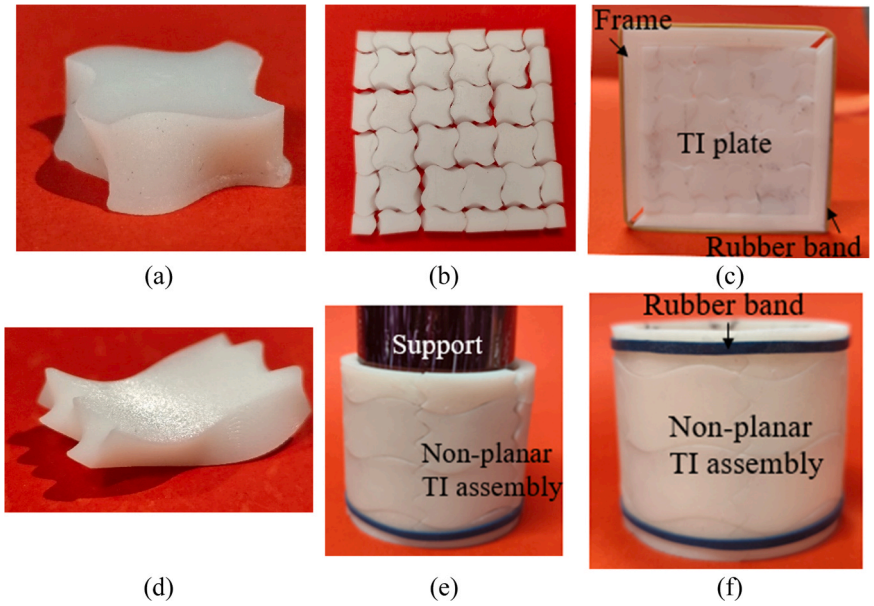

Fig. 14. Examples of 3D printed TI structures: (a) planar TI element, (b) positioning planar elements, (c) planar TI structure, (d) non-planar TI element, (e) positioning non-planar elements, and (f) tubular structure.

$a = 50$ mm, a height of $h = a/2 = 25$ mm, and a curve function defined by $f(x) = 6\sin 2\frac{\pi x}{a}(x \in [0, a])$. The curve function amplitudes for the other two designs are adjusted to ensure uniformity in height, volume, and interface morphology. The impact performance of $400 \times 400 \times 25$ mm TI concrete plates (compressive strength: 28.6 MPa) is simulated using LS-DYNA. A typical finite element model for the TI plates is shown in Fig. 15. Each plate is impacted by a rigid spherical indenter (25 mm diameter) at velocities ranging from 0.2 to 3.0 m/s. The boundary of each plate is confined by a steel frame subjected to a torque of 10 Nm. A 4 mm mesh size is applied across the plates. The concrete behaviour is modelled using the continuous surface cap model (CSCM), with failure defined by a maximum principal strain of 0.10. The steel frame is modelled with an elastic material model (MAT 001). Interactions between TI elements are simulated using "Automatic_Surface_To_Surface" contact with a friction coefficient of 0.4 for all concrete-to-concrete interfaces, while the interaction between the indenter and the TI structure is modelled using the same keyword but with a frictionless setting. These contact settings have been demonstrated to be reasonable in prior study [35].

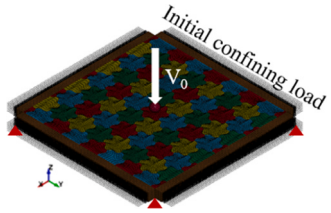

Fig. 15. Finite element model for typical TI plates.

3.3.1. *Effect of topological interlocking*

To demonstrate the influence of interlocking design on the structural performance of TI plates compared to a monolithic plate, Fig. 16 presents the relationship between energy dissipation and maximum indenter displacement, along with the effective stress distributions of the monolithic plate and a typical TI plate at a drop height of 1.0 m. The energy dissipation is calculated as the difference in kinetic energy of the indenter measured before and after its impact with the plate. As can be seen, compared to the monolithic plate, TI plates exhibit greater maximum indenter displacement and energy dissipation. The enhanced energy dissipation is directly linked to the higher displacement which

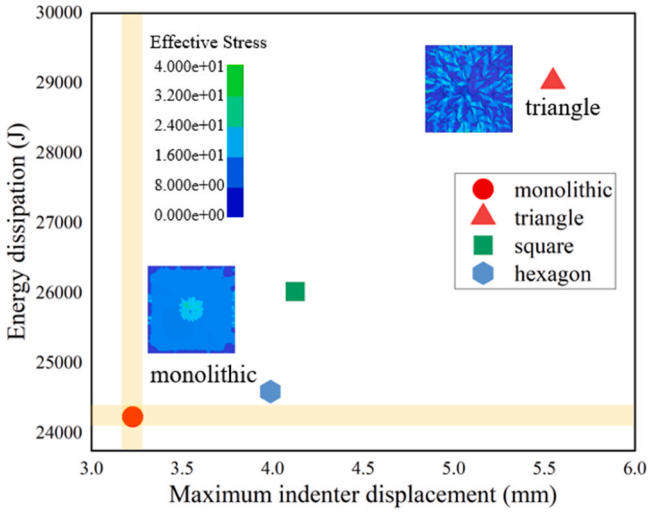

Fig. 16. Energy dissipation-maximum indenter displacement relationship for monolithic and TI plates at a 1 m drop height, and stress distributions on the bottom surfaces of monolithic and triangular-based plate.

allows the TI system to absorb more kinetic energy before failure. The enhanced energy dissipation can generally be attributed to two main factors: increased displacement and stress delocalisation. The segmentation and mobility of individual elements in TI structures allow for greater deformation, which is distributed across interfaces to enable controlled energy dissipation. This mechanism prevents sudden failure by converting impact energy into recoverable deformation energy, thereby improving resilience under dynamic loading. Additionally, unlike monolithic structures, TI designs delocalise stress and promote more uniform load distribution, enhancing material utilisation and energy dissipation efficiency, as evidenced by the stress patterns in the triangular TI plate (Fig. 16).

3.3.2. *Impact performance of TI structures at varying drop heights*

Fig. 17(a) shows the impact response of TI structures subjected to indenter impact from various drop heights. All results are normalised against those of a monolithic plate with identical dimensions and concrete material properties. In general, the relative energy dissipation of TI structures decreases with the increase of indenter drop height, exhibiting three distinct stages which are highlighted in different colours in Fig. 17(a). In the first stage, when the drop height is 0.5 m or lower, all TI plates exhibit superior energy dissipation compared to the monolithic plate, with the triangular-based configuration performing the best. At this stage, the relative maximum indenter displacement of the triangular-based plate increases with the indenter drop height, whereas the other two TI plates exhibit a decreasing trend. Nevertheless, all TI structures maintain values above 1.0, indicating a more compliant deformation mode. The enhanced energy dissipation and flexibility are primarily attributed to the segmentation and interlocking effect. Segmentation reduces stress concentration and promotes progressive failure, while interlocking enhances load redistribution and energy absorption through frictional sliding and constrained relative motion between elements. As the drop height increases beyond 0.5 m and up to 2.0 m, the relative energy dissipation of TI structures gradually decreases. The hexagonal-based TI plate exhibits energy dissipation close to that of the monolithic plate, whereas the other two TI plates still show enhanced energy dissipation. During this stage, the displacement of the triangular-based TI plate continues to increase, reaching its peak value at an indenter drop height of approximately 2.0 m, whereas the other two TI structures experience a slight decline in displacement. The segmented nature of TI structures enables greater global deformation; however, as deflection increases, the relative movement between elements intensifies, reducing contact and weakening inter-element interactions, which in turn diminishes the effectiveness of interlocking. When the drop height exceeds 2.0 m, the relative displacement of all TI plates decreases but remains above 1.0, while the relative energy dissipation values for the hexagonal-based and square-based TI structures drop below 1.0. This decline is primarily attributed to material failure, which becomes the dominant energy dissipation mechanism at higher impact energies. At this stage, the energy absorption process is governed by fracture rather than interlocking interactions. This shift in mechanism is evidenced by the development of larger cracks and the failure of central elements, as observed in Fig. 17(d).

Figs. 17(b) to 17(d) compare the stress and deflection contours of representative TI plates (with maximum and minimum relative energy dissipation) to those observed in the monolithic plate. At Stage I, the monolithic plate exhibits concentrated stress at the centre, whereas TI plates, particularly the one created based on triangular base polygon, show more distributed stress patterns. The deflection contours indicate a localised and smaller central deflection in the monolithic plate, while TI designs enable greater overall deformation and a more widespread distribution of deformation. Under low-velocity impact, the elements in TI plates maintain well-formed contact interfaces, facilitating effective inter-element interaction and material jamming. These mechanisms, involving the transfer of forces through interlocking elements and the redistribution of stress, lead to enhanced energy dissipation compared to the monolithic plate. At Stage II, the stress patterns in TI plates demonstrate increased concentrations along element interfaces, while the deflection contours show expanded deformation areas compared to the monolithic plate, highlighting how the segmented design enables more global deformation through relative movement between elements. Stage III is characterised by intense stress concentrations at the element interfaces and noticeable failure of central elements in TI structures. As the impact energy increases, the stress distribution in TI structures becomes increasingly chaotic, indicating a breakdown in the organised interaction between elements. At this stage, the energy absorption process transitions from being primarily driven by element interaction and compliant deformation to being dominated by material failure. This transition occurs as the deformation becomes too severe for the interlocking elements to maintain effective contact, leading to localised fracture and a significant reduction in the structure's ability to redistribute energy.

4. Discussion

4.1. *Parameterisation design method*

Compared to previous studies [2,18,36] that employed complex geometric or mathematical methods to control element shape, the design framework proposed in this paper simplifies the design process by establishing a direct and intuitive connection between design parameters and the resultant element shapes. The TI elements generated in this study and their interlocking effect are governed by four parameters, including the type of polygon tiling, polygon length, curve function, and element thickness. This design approach allows for rapid exploration of various alternatives by adjusting design parameters, thereby facilitating efficient design optimisation. The distinctive appeal of TI structures is rooted in their geometric characteristics. Researchers have delved into investigating the relationship between mechanical properties and geometric features [30,37,38]. The approach proposed in this study provides a robust framework for performance-oriented design and optimisation of TI structures. By leveraging the inherent geometric advantages, this method enhances the ability to fine-tune structural properties to meet specific performance criteria.

Additionally, the monomorphic nature of the TI elements generated in this study offers distinct advantages for manufacturing and construction practices. Despite the potential for higher manufacturing costs due to the complexity of element shapes, the monomorphic prototile requires only a one-time moulding, making it reusable. Furthermore, the

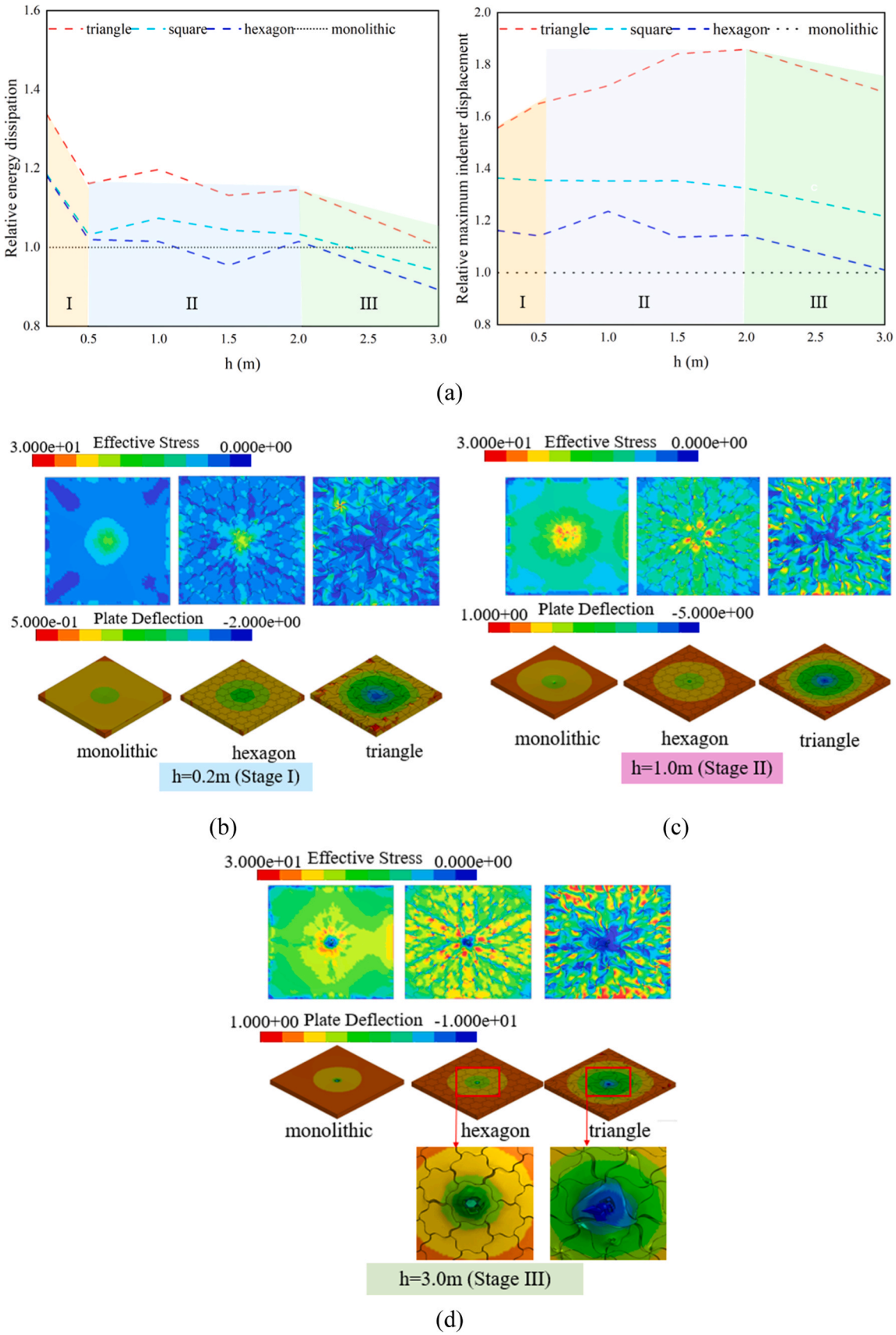

Fig. 17. Impact responses of monolithic and TI structures: (a) normalised energy dissipation and maximum indenter displacement at various indenter drop heights, and (b-d) comparisons of stress and deflection contours at drop heights of 0.2 m, 1 m, and 3 m.

uniformity interlocking nature of TI elements minimise assembly errors and reduce costs associated with bonding, connecting materials, and alignment. The streamlined assembly process has the potential to improve overall efficiency and contribute to more precise and reliable construction.

Numerical results presented in Section 3.3 demonstrate that specific design parameters, particularly the polygon shape, exert a sound influence on structural compliance and energy dissipation. These observations suggest a strong correlation between geometric configurations and the resulting mechanical performance of TI structures. Although the present study primarily focuses on establishing a geometric design framework and validating structural feasibility, the observed trends provide initial evidence of parameter-performance linkages. This work therefore serves as a foundational step toward the future development of performance-driven design strategies and optimisation.

4.2. Geometric flexibility in TI element design

In this paper, several TI element designs are presented as examples. However, the proposed approach offers a vast range of design possibilities by integrating various plane tilings, curve functions, and contact surface morphologies. Given that numerous polygon shapes can tessellate the plane [39], there exists a rich selection of prototiles for developing TI elements. Furthermore, alternative curve functions, such as circular, wavy polynomial, and square wave functions, which introduce protrusions and recesses, can be used to modify edge shapes. Besides, other curve representation methods like the Bezier curve that controls the shape by changing the positions of control points, can also offer more design alternatives. Despite these possibilities, as demonstrated in Section 3.3.2, certain geometric configurations, such as hexagonal tiles, exhibit less favourable mechanical responses. This highlights that the effectiveness of each design must be evaluated based on its mechanical performance rather than simply its geometric variety. The relationship between the TI element geometry and the overall mechanical performance warrants further exploration.

4.3. Shaping strength with geometry: the interlocking blueprint

The comparison of impact responses between monolithic and TI structures highlights the significant role of interlocking on structural performance. The segmentation and element interactions enhance compliant deformation and energy absorption. However, as deformation increases, damage initiates and intensifies, weakening the interlocking effect. At this stage, the energy absorption mechanism shifts from being primarily governed by element interactions and compliant deformation to being dominated by material failure. Furthermore, as demonstrated in Section 3.3, the morphology of TI elements plays a crucial role in interlocking efficiency. Triangular-based configurations exhibit superior energy absorption due to improved contact engagement and more effective stress distribution. In contrast, hexagonal-based design does not provide a significant advantage under high-impact energy conditions. This study highlights the influence of geometric design on mechanical behaviour, providing a foundation for further research to refine and optimise interlocking-based structural systems.

5. Conclusions

This paper proposes a versatile framework for designing topological interlocking (TI) elements with curved contact surfaces, significantly expanding their geometric and structural possibilities. The method involves three key steps: 1) selecting monomorphic polygonal prototiles, 2) shaping edges with curve functions to form concavo-convex features, and 3) creating curved interfaces to ensure self-aligning assembly and robust interlocking. This approach enables the creation of new TI elements based on various polygonal tilings and edge curve functions, with interlocking achieved through matched concavo-convex surface morphology. The geometry of TI elements is governed by four parameters: polygonal prototile type, edge length, curve function, and element thickness. The proposed approach enables the design of both planar and non-planar TI structures. To demonstrate the effectiveness of the generalised framework, 24 planar and 12 non-planar TI elements are designed, and the feasibility of the designed TI structures is further validated through two 3D-printed prototypes representing both planar and non-planar structures. The investigation of the impact performance of TI structures confirms their superior energy dissipation capacity compared to monolithic plates, particularly under lower impact energies. The interlocking mechanism enhances energy dissipation through inter-element interactions, stress delocalisation, and a more compliant deformation mode. To enable performance-driven design and practical implementation, a deeper understanding of the relationship between geometric parameters and mechanical behaviour is essential. Future studies will systematically evaluate how design parameters, including polygon shape, size, and curve function, affect the structural performance of TI assemblies. Such efforts are critical for developing robust design guidelines and optimisation strategies tailored to engineering requirements and loading scenarios.

TI structures offer practical advantages, especially in applications requiring energy dissipation, damage tolerance, and modularity. Promising applications include impact- or blast-resistant panels, where inter-element motion helps prevent catastrophic failure, as well as architectural facades and pavements benefiting from dry assembly and adaptability. In seismic design, their ability to accommodate relative movement while preserving global integrity is particularly valuable. While confinement requirements may pose challenges, however, passive strategies like gravitational confinement offer feasible solutions. Future research should explore practical confinement methods to facilitate broader implementation. Furthermore, the potential to increase toughness and control crack propagation through material selection offers promising avenues for future research. By incorporating graded or ductile materials, it is expected that the crack arresting behaviour and energy absorption capacity can be enhanced. Additionally, optimising the interface morphology to control crack propagation paths will also be explored to prevent catastrophic failure. Apart from that, a key focus of future work will be the examination of the mechanical behaviour of non-planar TI structures, extending the findings of the current study to broader, more complex structural applications.

CRediT authorship contribution statement

Siya Wang: Writing – review & editing, Writing – original draft, Validation, Methodology, Investigation, Formal analysis, Data curation, Conceptualization. **Y.X. Zhang:** Writing – review & editing, Supervision, Methodology. **Xiaoshan Lin:** Writing – review & editing, Validation, Supervision, Resources, Methodology, Investigation, Funding acquisition, Conceptualization. **Yi Min Xie:** Writing – review & editing, Supervision, Methodology, Investigation, Conceptualization.

Declaration of Competing Interest

The authors declare that they have no known competing financial interests or personal relationships that could have appeared to influence the work reported in this paper

Acknowledgment

The authors gratefully acknowledge the financial support provided by the Australian Research Council (FT240100301).

Data availability

Data will be made available on request.

References

[1] Molotnikov A, Estrin Y, Dyskin AV, Pasternak E, Kanel-Belov AJ. Percolation mechanism of failure of a planar assembly of interlocked osteomorphic elements. Eng Fract Mech May 2007;74(8):1222–32. https://doi.org/10.1016/j.engfracmech.2006.07.012.

[2] Dyskin AV, Estrin Y, Pasternak E, Khor HC, Kanel-Belov AJ. Fracture Resistant Structures Based on Topological Interlocking with Non-planar Contacts. Adv Eng Mater Mar. 2003;5(3):116–9. https://doi.org/10.1002/adem.200390016.

[3] Ross BE, Yang C, Kleiss MCB, Okumus P, Elhami Khorasani N. Tessellated structural-architectural systems: concept for efficient construction, repair, and disassembly. J Archit Eng Sep. 2020;26(3):04020020. https://doi.org/10.1061/(ASCE)AE.1943-5568.0000418.

[4] Mirkhalaf M, Zhou T, Barthelat F. Simultaneous improvements of strength and toughness in topologically interlocked ceramics. Proc Natl Acad Sci Sep. 2018;115(37):9128–33. https://doi.org/10.1073/pnas.1807272115.

[5] Mirkhalaf M, Sunesara A, Ashrafi B, Barthelat F. Toughness by segmentation: Fabrication, testing and micromechanics of architectured ceramic panels for impact applications. Int J Solids Struct Feb. 2019;158:52–65. https://doi.org/10.1016/j.ijsolstr.2018.08.025.

[6] Schaare S, Riehemann W, Estrin Y. Damping properties of an assembly of topologically interlocked cubes. Mater Sci Eng: A Sep. 2009;521–522:380–3. https://doi.org/10.1016/j.msea.2008.10.069.

[7] C. Khor, A.V. Dyskin, E. Pasternak, Y. Estrin, and A.J. Kanel–Belov, "Integrity and fracture of plate–like assemblies of topologically interlocked elements," pp. 449–456, Jan. 2002.

[8] H.T.D. Yong, 'Utilisation of topologically-interlocking osteomorphic blocks for multi-purpose civil construction', 2011. Accessed: Apr. 28, 2024. [Online]. Available: ⟨https://research-repository.uwa.edu.au/en/publications/utilisation-of-topologically-interlocking-osteomorphic-blocks-for⟩.

[9] Jamshidi A, et al. State-of-the-art of interlocking concrete block pavement technology in Japan as a post-modern pavement. Constr Build Mater Mar. 2019;200:713–55. https://doi.org/10.1016/j.conbuildmat.2018.11.286.

[10] Khudyakov M, Dyskin AV, Pasternak E. Continuum model of wave propagation in fragmented media: linear damping approximation. Nonlinear Process Geophys Aug. 2017;24(3):461–6. https://doi.org/10.5194/npg-24-461-2017.

[11] Xu W, Lin X, Li P, Wu Y-F, Xie YM. Impact behaviour of tunnel lining assembled from non-planar interlocking steel fibre reinforced concrete bricks. Eng Struct Dec. 2023;296:116907. https://doi.org/10.1016/j.engstruct.2023.116907.

[12] Estrin Y, Dyskin AV, Pasternak E. Topological interlocking as a material design concept. Mater Sci Eng C Aug. 2011;31(6):1189–94. https://doi.org/10.1016/j.msec.2010.11.011.

[13] Dyskin AV, Estrin Y, Kanel-Belov AJ, Pasternak E. Interlocking properties of buckyballs. Phys Lett A Dec. 2003;319(3–4):373–8. https://doi.org/10.1016/j.physleta.2003.10.027.

[14] Dyskin AV, Estrin Y, Kanel-Belov AJ, Pasternak E. Topological interlocking of platonic solids: A way to new materials and structures. Philos Mag Lett Jan. 2003;83(3):197–203. https://doi.org/10.1080/0950083031000065226.

[15] M. Weizmann, O. Amir, and Y.J. Grobman, 'Topological Interlocking in Architectural Design', presented at the CAADRIA 2015: Emerging Experience in Past, Present and Future of Digital Architecture, Daegu, Taiwan, 2015, pp. 107–116. doi: 10.52842/conf.caadria.2015.107.

[16] Bejarano A, Hoffmann C. A generalized framework for designing topological interlocking configurations. Int J Archit Comput Mar. 2019;17(1):53–73. https://doi.org/10.1177/1478077119827187.

[17] Dyskin AV, Estrin Y, Pasternak E. Topological Interlocking Materials. in Springer Series in Materials Science, vol. 282. In: Estrin Y, Bréchet Y, Dunlop J, Fratzl P, editors. Architectured Materials in Nature and Engineering, 282. Cham: Springer International Publishing; 2019. p. 23–49. https://doi.org/10.1007/978-3-030-11942-3_2. in Springer Series in Materials Science, vol. 282.

[18] Rezaee Javan A, Seifi H, Xu S, Ruan D, Xie YM. The impact behaviour of plate-like assemblies made of new interlocking bricks: An experimental study. Mater Des Nov. 2017;134:361–73. https://doi.org/10.1016/j.matdes.2017.08.056.

[19] Akleman E, et al. Generalized abeille tiles: Topologically interlocked space-filling shapes generated based on fabric symmetries. Comput Graph Jun. 2020;89:156–66. https://doi.org/10.1016/j.cag.2020.05.016.

[20] Koureas I, Pundir M, Feldfogel S, Kammer DS. The key to the enhanced performance of slab-like topologically interlocked structures with non-planar blocks. Int J Solids Struct Dec. 2023;285:112523. https://doi.org/10.1016/j.ijsolstr.2023.112523.

[21] Koureas I, Pundir M, Feldfogel S, Kammer DS. Beam-like topologically interlocked structures with hierarchical interlocking. J Appl Mech Aug. 2023;90(8):081008. https://doi.org/10.1115/1.4062348.

[22] Dalaq AS, Barthelat F. Manipulating the geometry of architectured beams for maximum toughness and strength. Mater Des Sep. 2020;194:108889. https://doi.org/10.1016/j.matdes.2020.108889.

[23] Xu W, Lin X, Xie YM. A novel non-planar interlocking element for tubular structures. Tunn Undergr Space Technol Sep. 2020;103:103503. https://doi.org/10.1016/j.tust.2020.103503.

[24] Kanel-Belov A, Dyskin A, Estrin Y, Pasternak E, Ivanov-Pogodaev I. Interlocking of convex polyhedra: towards a geometric theory of fragmented solids. MMJ 2010;10(2):337–42. https://doi.org/10.17323/1609-4514-2010-10-2-337-342.

[25] Dyskin AV, Estrin Y, Pasternak E, Khor HC, Kanel-Belov AJ. The principle of topological interlocking in extraterrestrial construction. Acta Astronaut Jul. 2005;57(1):10–21. https://doi.org/10.1016/j.actaastro.2004.12.005.

[26] P. Cutellic, U. Frick, T. Grabner, and R. Maleczek, 'Aggregation of Polyhedron Modules on a Freeform Surface', *International Conference On Geometry and Graphic*, 2014.

[27] Weizmann M, Amir O, Grobman YJ. Topological interlocking in architecture: a new design method and computational tool for designing building floors. Int J Archit Comput Jun. 2017;15(2):107–18. https://doi.org/10.1177/1478077117714913.

[28] Weizmann M, Amir O, Grobman YJ. Topological interlocking in buildings: a case for the design and construction of floors. ', Autom Constr Dec. 2016;72:18–25. https://doi.org/10.1016/j.autcon.2016.05.014.

[29] Krishnamurthy V, et al. Layerlock: layer-wise collision-free multi-robot additive manufacturing using topologically interlocked space-filling shapes. Comput -Aided Des Nov. 2022;152:103392. https://doi.org/10.1016/j.cad.2022.103392.

[30] Weizmann M, Amir O, Grobman YJ. The effect of block geometry on structural behavior of topological interlocking assemblies. ', Autom Constr Aug. 2021;128:103717. https://doi.org/10.1016/j.autcon.2021.103717.

[31] Grünbaum B, Shephard GC. Tilings and Patterns. Courier Dover Publications; 1987.

[32] Boni C, Ferretti D, Lenticchia E. Effects of brick pattern on the static behavior of masonry vaults. Int J Archit Herit Aug. 2022;16(8):1199–219. https://doi.org/10.1080/15583058.2021.1874565.

[33] R. Chick and C. Mann, "Equilateral k-Isotoxal Tiles," 2012. Accessed: Apr. 28, 2024. [Online]. Available: ⟨https://faculty.washington.edu/cemann/equilateral-isotoxal.pdf⟩.

[34] Anycubic Photon M3 Max," *ANYCUBIC-US*, 2024. ⟨https://store.anycubic.com/products/photon-m3-max⟩ (accessed Sep. 18, 2024).

[35] Rezaee Javan A, Seifi H, Xu S, Lin X, Xie YM. Impact behaviour of plate-like assemblies made of new and existing interlocking bricks: a comparative study. Int J Impact Eng Jun. 2018;116:79–93. https://doi.org/10.1016/j.ijimpeng.2018.02.008.

[36] Kanel-Belov A, Dyskin A, Estrin Y, Pasternak E, Ivanov-Pogodaev I. Interlocking of convex polyhedra: towards a geometric theory of fragmented solids. Mosc Math J 2010;10(2):337–42. https://doi.org/10.17323/1609-4514-2010-10-2-337-342.

[37] Carlesso M, et al. Enhancement of sound absorption properties using topologically interlocked elements. Scr Mater Apr. 2012;66(7):483–6. https://doi.org/10.1016/j.scriptamat.2011.12.022.

[38] E. Mousavian, C. Casapulla, and K. Bagi, "The influence of geometry on the frictional sliding of ∧ and ∨ shaped interlocking joints in masonry assemblages," Accessed: Apr. 28, 2024. [Online]. Available: ⟨https://www.research.ed.ac.uk/en/publications/the-influence-of-geometry-on-the-frictional-sliding-of-and-shaped⟩.

[39] Robbin, J.W., "Guide for First-Time Instructors: For Course on Modeling with Differential Equations", 2006, Accessed: Jul. 24, 2024. [Online]. Available: ⟨https://people.math.wisc.edu/~jwrobbin/141dir/propp/COMAP/Guidefor1stTimeInstructors/u_FAPP07_FTI_20.pdf⟩.